A Miniaturized 90° Schiffman Phase Shifter with Open-Circuited Trans-Directional Coupled Lines

Yuan Cao[1, 2], Zhongbao Wang[1, 3, *], Shaojun Fang[1], and Yuanan Liu[3]

Abstract—A symmetrical open-circuited $\lambda/4$ trans-directional (TRD) coupled line is proposed to replace the $3\lambda/4$ reference line of an existing 90° Schiffman phase shifter for miniaturization. The coupling factor of the TRD coupled line can be used to control input matching and phase ripple, which adds an additional optimization variable to the design of a Schiffman phase shifter. There are two transmission zeros near the operational frequency band, which can be used to suppress adjacent frequency interferences and accompanies two phase leaps so that the realizable bandwidth is about $28 \sim 42\%$. Simulated and measured results are given to verify the proposed method.

1. INTRODUCTION

90° differential phase shifters are widely used in feeding networks of broadband circularly polarized antennas such as dual- or quadri-feed patch antennas [1], crossed dipoles [2] and dielectric resonator antennas [3]. A classical design of a 90° differential phase shifter is the Schiffman phase shifter [4], which is a four-port network consisting of two separate circuit parts: the main and reference lines. In an ideal case, the connection part of input and output ports should be zero in length. The main line only comprises a symmetrical $\lambda/4$ coupled-line section connected together at one end to generate a phase shift equal to 180°. The reference line is a section of a $3\lambda/4$ uniform transmission line (TL) producing a phase shift equal to 270°. The design requirement of a phase shifter is to ensure that the differential phase shift between the two lines $\Delta\psi$ is equal to 90° with an acceptable phase ripple over the operating bandwidth. In order to broaden the operating bandwidth, the design requires a tight coupling in the coupled-line section, which cannot always be implemented with printed circuit board (PCB) fabrication technology [5]. Therefore, a floating conductor [6] and slots [7] on the ground plane were introduced to increase the level of coupling in the parallel-coupled microstrip lines for realizing a broadband 90° Schiffman phase shifter [8]. However, with the increase of the slot width, the insertion loss is significantly increased. On the other hand, there is no synthesis formula available to design the coupled structure. Usually, the design of a coupled structure was accomplished using commercial full-wave electromagnetic simulators through a trial-and-error iterative process [6]. The simulation methods without any design guidelines are time consuming and may not lead to the optimum solutions. Thus, an optimization methodology for the development of microwave circuits and antennas [9–12] can be used to achieve the optimum performance.

Recently, improved broadband 90° Schiffman phase shifters were proposed by using the parallel coupled microstrip lines loaded with an open- or short-circuited stub [13, 14]. However, all the 90° Schiffman phase shifters [4–8, 13, 14] and other 90° differential phase shifters with broadside coupling
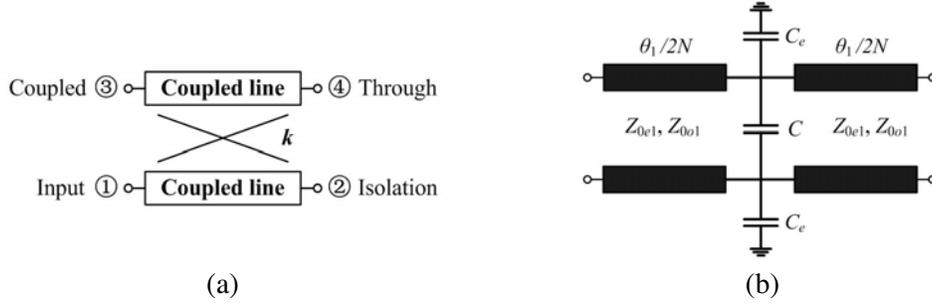
Figure 1. Topology of the TRD coupler. (a) Schematic of the TRD coupler. (b) One unit cell of capacitor-loaded coupled lines.

structures [15], double microstrip-slot transitions [16], and TLs loaded open- or short-circuited stubs [17–19] require long reference lines (i.e., $3\lambda/4$) which are difficult to miniaturize. In order to alleviate this problem, an open-circuited U-type coupled line was presented to replace the reference line [20]. However, the U-type coupled line with an asymmetrically open-circuited end requires even- and odd-mode velocities compensation structures (e.g., slots in coupled strip).

The trans-directional (TRD) coupled line shown in Figure 1 was firstly introduced with periodically capacitor-loaded coupled microstrip lines by Shie et al. [21]. One important advantage of the TRD coupled line is that it is easy to implement tight coupling (e.g., 3 dB) with weak coupled microstrip lines. Another advantage is that the through and coupled ports of the TRD coupled line are on the same conductor strip, which is different from traditional parallel-coupled lines. When the through and coupled ports are connected with open loads, the input and output ports of the $\lambda/4$ TRD coupled line is also on the same conductor strip as a result of a small insertion loss and produces a phase shift equal to $90°$. Thus, the open-circuited $\lambda/4$ TRD coupled line was introduced to replace the $3\lambda/4$ reference line for realizing a miniaturized $90°$ differential phase shifter in this paper. Details of the phase shifter design and both the theoretical and experimental results are given and discussed.

2. CIRCUIT STRUCTURE AND DESIGN THEORY

Figure 2 shows the proposed configuration of the modified $90°$ Schiffman phase shifter. The main line is the same as a traditional $90°$ Schiffman phase shifter. The reference line consists of a TRD coupler with the through and coupled ports connected with open loads.

To analyze this phase shifter, we first introduce a TRD coupler, the schematic of which is illustrated in Figure 1. Note that the locations of its isolation and through ports are the opposite of those of a parallel-coupled microstrip coupler. Based on the analysis of the TRD coupler in [21], S-parameters of the TRD coupler is

$$S_{\text{TRD}} = \begin{bmatrix} 0 & 0 & k & -j\sqrt{1-k^2} \\ 0 & 0 & -j\sqrt{1-k^2} & k \\ k & -j\sqrt{1-k^2} & 0 & 0 \\ -j\sqrt{1-k^2} & k & 0 & 0 \end{bmatrix} \tag{1}$$

where k represents the coupling factor of TRD coupler at the coupled port.

According to the modified reference line configuration in Figure 2, the open-circuited TRD coupled line can be analyzed with S-parameters of the TRD coupler. Referring to Figure 1(a), when only port 1 is input, and the normalization value is 1, there is no output signal at port 2, and the outputs of ports 3 and 4 are k and $-j\sqrt{1-k^2}$, respectively. Then, total reflection signals of open loads at ports 3 and 4 turn into the TRD coupler. At last, port 2 has an output signal of $-j2k\sqrt{1-k^2}$ and the phase of which is lagged $90°$ with respect to the input signal at port 1, and the reflection signal at port 1 is $2k^2 - 1$. When the TRD coupler is a 3-dB coupler (i.e., $k = 1/\sqrt{2}$), the reflection signal at port 1 is equal to zero (an ideal input matching is obtained). In order to realize a wideband $90°$ phase shifter, coupling
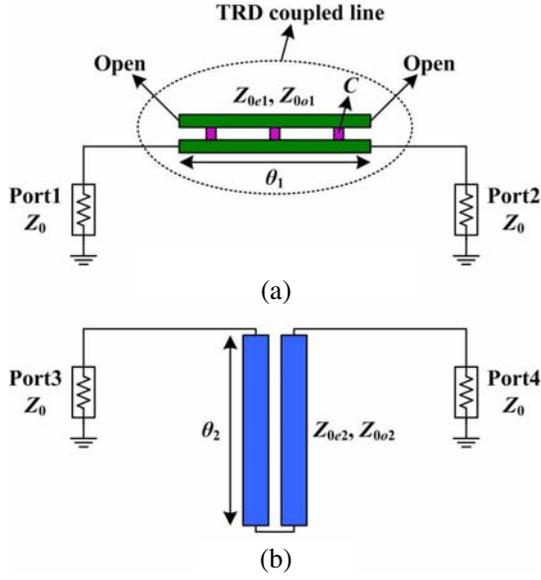
Figure 2. Configuration of the proposed differential phase shifter. (a) Modified reference line. (b) Main line.
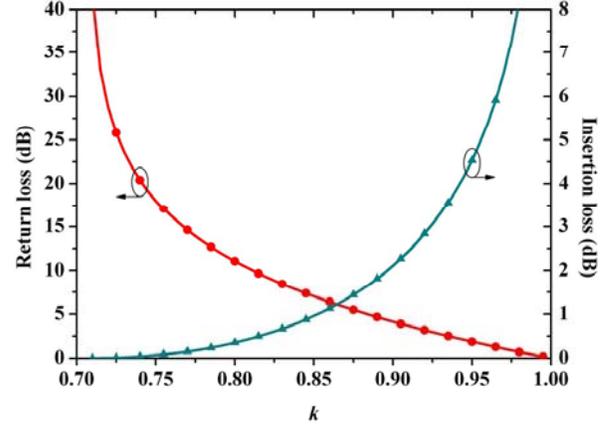
Figure 3. Return and insertion losses of the modified reference line versus coupling factor k of the TRD coupled line.

factor k of the TRD coupled line needs to be increased, but the input matching is deteriorated with the increase of k as shown in Figure 3. When the return loss in the operating frequency band is required to be greater than 10 dB, and the coupling factor k is less than 0.81 with insertion loss less than 0.45 dB. Thus, there is a trade-off between the input matching and bandwidth of the proposed 90° phase shifter by choosing a proper value of k. When coupling factor k of the TRD coupled line is chosen, the even- and odd-mode analysis can be used to determine the coupled line impedance Z_{0e1}, Z_{0o1}, and the loaded capacitor C of the TRD coupled line, as shown in Figure 2(a).

According to the even- and odd-mode analysis in [21], the impedance Z_{0e1}, Z_{0o1}, loaded capacitor C_e, and C of the cells of the TRD coupler, as shown in Figure 1(b), can be derived as

$$Z_{0e1} = \frac{Z_0 \sqrt{(1+k)/(1-k)}}{\sqrt{\dfrac{2\sin(\theta_1/N) + b_e \cos(\theta_1/N) - b_e}{2\sin(\theta_1/N) + b_e \cos(\theta_1/N) + b_e}}} \tag{2}$$

$$Z_{0o1} = \frac{Z_0 \sqrt{(1-k)/(1+k)}}{\sqrt{\dfrac{2\sin(\theta_1/N) + b_o \cos(\theta_1/N) - b_o}{2\sin(\theta_1/N) + b_o \cos(\theta_1/N) + b_o}}} \tag{3}$$

$$C_e = \frac{b_e}{\omega Z_{0e1}} \tag{4}$$

$$C = \frac{1}{2}\left(\frac{b_o}{\omega Z_{0o1}} - \frac{b_e}{\omega Z_{0e1}}\right) \tag{5}$$

$$b_e = \frac{2\left(\cos\dfrac{\theta_1}{N} - \cos\dfrac{\pi}{2N}\right)}{\sin\dfrac{\theta_1}{N}} \tag{6}$$

$$b_o = \frac{2\left(\cos\dfrac{\theta_1}{N} - \cos\dfrac{3\pi}{2N}\right)}{\sin\dfrac{\theta_1}{N}} \tag{7}$$

where parameters N, k, and θ_1 mean the number of cells, coupling factor, and electrical length of the coupled-line, respectively. According to [21], the larger the number of sections is used in the design of the TRD coupler, the wider the operation bandwidth is. It also mentions that the bandwidth increase is very small when the number of cells changes from three to six or more, and the outputs of the through and coupled ports will deteriorate as the number of cells becomes larger. Thus, a three-cell design is selected as a compromise between bandwidth and insertion loss. Furthermore, Equations (4) and (6) imply that the loaded capacitor C_e becomes zero when the electrical length of the coupled-line θ_1 equals $\pi/2$. Thus, $\lambda/4$ coupled line is adopted in this design to remove C_e so that circuit complexity can be reduced.

The main line in Figure 2 is an all-pass network when the following relation is satisfied [22].

$$Z_0 = \sqrt{Z_{0e2}Z_{0o2}} \tag{8}$$

Meanwhile,

$$S_{33} = S_{44} = 0 \tag{9}$$

$$S_{43} = S_{34} = \frac{Z_{0e2}\cot\theta_2 + Z_{0o2}\tan\theta_2}{Z_{0e2}\cot\theta_2 - Z_{0o2}\tan\theta_2 + j2Z_0} = e^{j\psi} \tag{10}$$

$$\psi = \arccos\left(\frac{g - \tan^2\theta_2}{g + \tan^2\theta_2}\right) \tag{11}$$

$$g = \frac{Z_{0e2}}{Z_{0o2}} \tag{12}$$

where θ_2, Z_{0e2}, Z_{0o2} mean the electrical length, and even- and odd-mode characteristic impedances of the coupled-line shown in Figure 2(b), respectively.

The phase difference of the phase shifter at the center operating frequency can be calculated as follows:

$$\Delta\psi = \text{phase}(S_{21}) - \text{phase}(S_{43}) = -90° - \psi \tag{13}$$

Equation (12) means that the phase difference $\Delta\psi$ at the center operating frequency only depends on the main line. Nevertheless, the bandwidth lies on the whole circuit. When the length of the main coupled-line also is chosen to be $\lambda/4$, it produces a phase shift of $\Delta\psi = -180°$. Then, the phase difference $\Delta\psi$ at the center operating frequency equals 90°. Thus, a miniaturized 90° phase shifter is achieved.

3. PARAMETERS ANALYSIS

Based on the previous theoretical analysis, the electrical parameters of the proposed circuit can be easily calculated with Equations (2)–(8) and (11)–(13). For observation of the effect of the electrical parameters, the Advanced Design System (ADS) circuit simulator will be used to analyze the proposed phase shifter in this section.

3.1. Effect of the Coupling Factor of the TRD Coupled Line

Figure 4 gives the effect of the coupling factor k of the TRD couple line on S-parameters of the proposed 90° phase shifter with $g = 1.0$, $\theta_1 = \pi/2$, and $\theta_2 = \pi/2$. It is observed that the coupling factor k of the TRD couple line shows a significant effect on the input matching (i.e., S_{11}) of the reference line at the centre operating frequency of 1 GHz. With the increase of k from 0.71 to 0.80, the impedance bandwidth for $|S_{11}| < -10$ dB is enhanced from 33.6% to 42.1%, as shown in Figure 5. However, over coupling (i.e., $k > 0.81$) will deteriorate the input matching at the centre operating frequency. Figure 4(b) gives the effect of k on the phase difference responses of the proposed 90° phase shifter. With the increase of

k from 0.71 to 0.80, the phase bandwidths for $90° \pm 10°$ is enhanced from 32.6% to 39.6% and that for $90° \pm 5°$ from 28.0% to 37.2%. Furthermore, it is seen from Figure 4 that there are two transmission zeros accompanying two phase leaps near 0.73 GHz and 1.23 GHz, respectively, which can be used to suppress adjacent frequency interferences and implies that the bandwidth of the proposed $90°$ phase shifter will be less than 50%.

3.2. Effect of the Even- and Odd-Mode Impedance Ratio of the Main Coupled Line

Figure 6 gives the effect of the even- and odd-mode impedance ratio g of the main coupled line on the phase difference responses of the proposed $90°$ phase shifter with $k = 0.8$, $\theta_1 = \pi/2$, and $\theta_2 = \pi/2$. It is found that increasing g causes greater phase ripple, which is similar to traditional $90°$ Schiffman phase shifter. When g is increased from 1.0 to 1.6, the phase bandwidth for $90° \pm 10°$ is improved from 39.6% to 42.2%.

Based on the analysis of Figures 4 and 6, the maximum realizable bandwidth of the proposed $90°$ phase shifter is about 42%, which is less than that of the existing $90°$ phase shifter [6–8, 13–19]. However, the length of the reference line is reduced by two thirds, and practical applications require a moderate bandwidth such as the Global Position System (GPS operation at the frequency band of 1.164–1.587 GHz covering L1, L2 and L5 bands, the fractional bandwidth of 30.8%) and ultra-high frequency (UHF) Radio Frequency Identification (RFID at 840–960 MHz, 13.3%).

4. IMPLEMENTATION AND PERFORMANCE

The analytical solutions and parameter analyses have been theoretically explained in Sections 2 and 3. In order to further validate the proposed $90°$ phase shifter experimentally, a $90°$ phase shifter with port characteristic impedance $Z_0 = 50\,\Omega$ for the GPS application is designed and implemented on a 1.5 mm-thick substrate with relative dielectric constant $\varepsilon_r = 2.65$. The example is designed by using microstrip realization technology with complete ground plane in the bottom layer, and the operating frequency is centered at 1.375 GHz.

In the design of the $90°$ phase shifter, the coupling factor of the TRD couple line is selected as $k = 0.728$ for return loss more than 24 dB at the centre operating frequency and $\theta_1 = \pi/2$ to remove loaded capacitor C_e for reducing circuit complexity. Using Equations (2)–(7), the circuit electrical parameters for the TRD couple line are obtained as $Z_{0e1} = 126.0\,\Omega$, $Z_{0o1} = 74.0\,\Omega$, and $C = 2.7$ pf. For the main coupled line with $\theta_2 = \pi/2$, the even- and odd-mode impedance ratio g is tuned with ADS circuit simulator to obtain an appropriate bandwidth with a smaller phase ripple and determined as
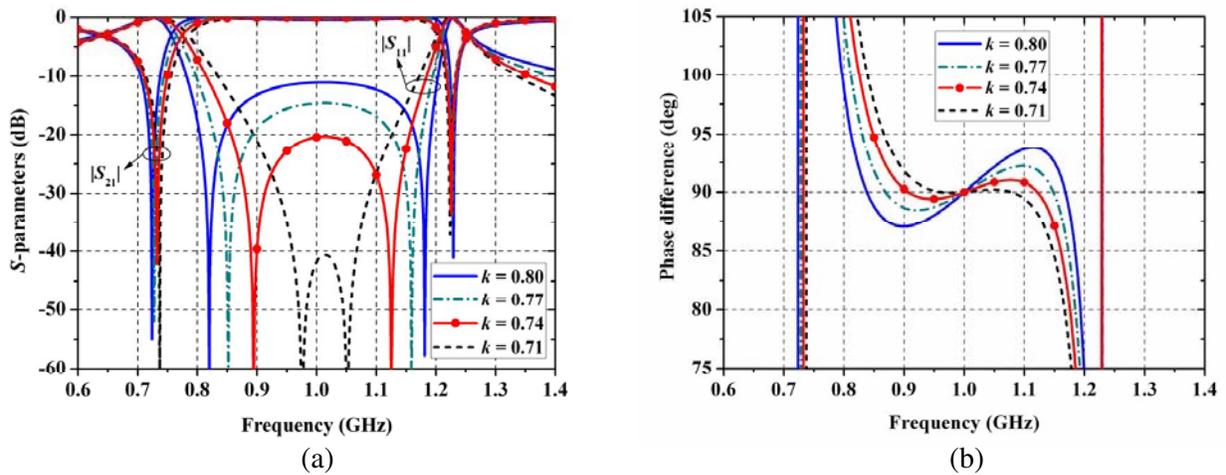
Figure 4. Effect of k on the S-parameters of the proposed $90°$ phase shifter. (a) Amplitude responses. (b) Phase responses.
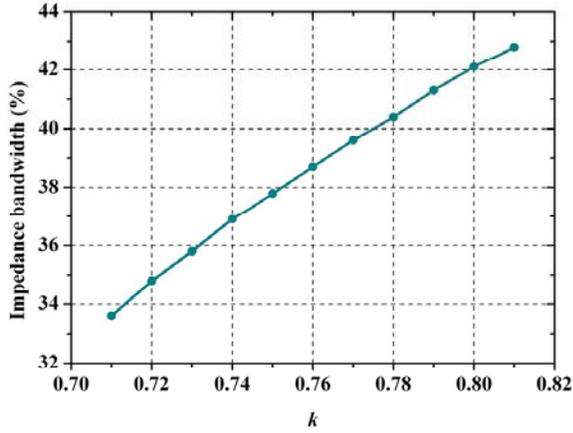
Figure 5. Effect of k on the impedance bandwidths for $|S_{11}| < -10\,\text{dB}$ of the proposed $90°$ phase shifter.
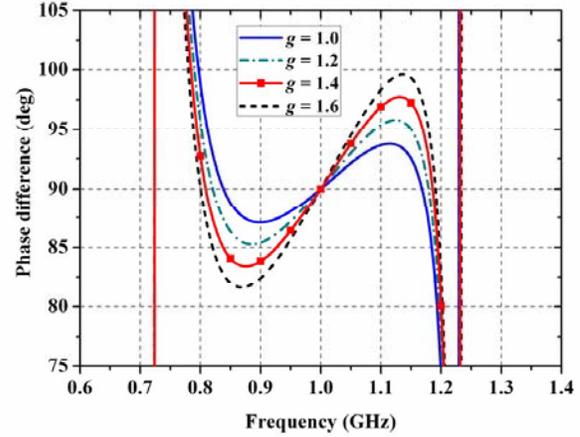
Figure 6. Effect of g on the phase difference responses of the proposed $90°$ phase shifter.
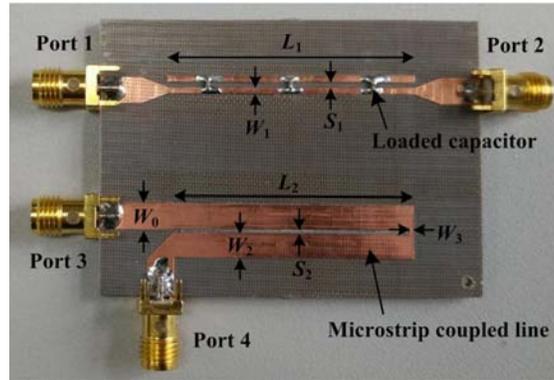
Figure 7. Photograph of the proposed $90°$ phase shifter.

$g = 1.55$. Using Equations (8) and (12), the even- and odd-mode impedances of the main coupled line are $Z_{0e2} = 62.2\,\Omega$ and $Z_{0o2} = 40.2\,\Omega$, respectively. Then, using the transmission line (TL) synthesis tool ADS *Linecalc*, the physical dimensions of TLs are calculated. However, optimal physical dimensions of TLs must take account of the discontinuous interfaces including the distributed capacitance effect of the open stubs at the ends. Therefore, the HFSS EM software is used to obtain the final dimensions. At last, the final dimensions of the $90°$ phase shifter are found and implemented as follows: $W_0 = 4.07\,\text{mm}$, $W_1 = 1.04\,\text{mm}$, $W_2 = 3.73\,\text{mm}$, $W_3 = 0.50\,\text{mm}$, $S_1 = 0.76\,\text{mm}$, $S_2 = 0.60\,\text{mm}$, $L_1 = 37.5\,\text{mm}$, and $L_2 = 37.1\,\text{mm}$. A photograph of the fabricated $90°$ phase shifter is shown in Figure 7. The overall dimension of the circuit is $58\,\text{mm} \times 42\,\text{mm}$ (around $0.39\lambda_g \times 0.29\lambda_g$, where λ_g is the guided wavelength of 50-Ω TLs at the center operating frequency).

To validate the design, S-parameter of the fabricated phase shifter is measured with an Agilent N5230A network analyzer. Figure 8 gives the simulated and measured S-parameters amplitude and phase difference responses of the proposed $90°$ phase shifter, respectively. From the measured results, it can be seen that the 10-dB return loss bandwidth is 33.3% from 1.133 to 1.587 GHz with insertion loss less than 1.4 dB, and the 3-dB insertion loss bandwidth is 39.4% from 1.077 to 1.606 GHz. The phase derivation is within $\pm 5°$ covering a band from 1.136 to 1.584 GHz, or 32.9% bandwidth. A $\pm 10°$ phase deviation can be obtained from 1.114 to 1.598 GHz or about 35.7% bandwidth, which is greater than the required bandwidth of 30.8% for GPS applications. There are some discrepancies between the simulated and measured results, which are mainly due to inaccurate values of the adopted 2.7-pF
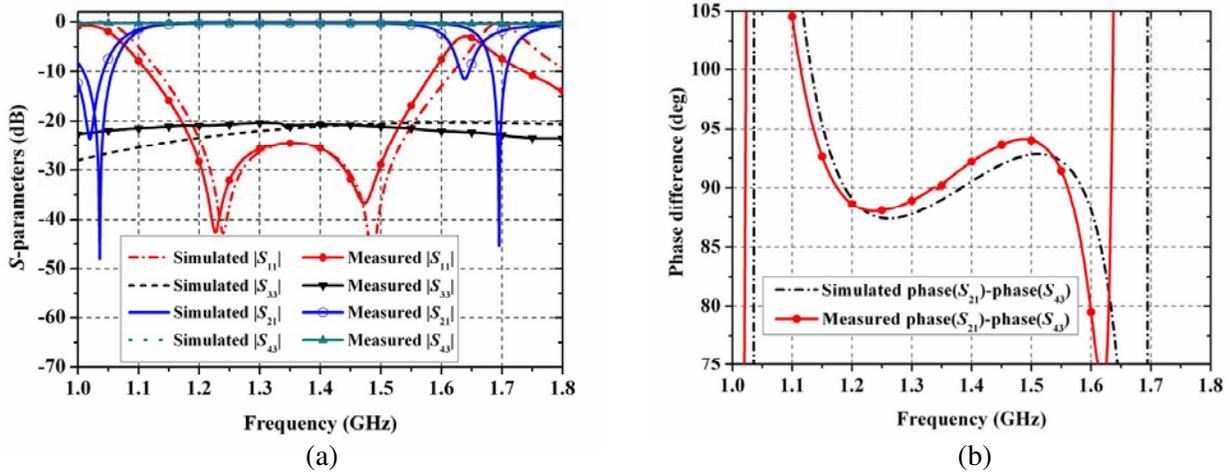
Figure 8. Simulated and measured S-parameters of the proposed $90°$ phase shifter. (a) Amplitude responses. (b) Phase responses.
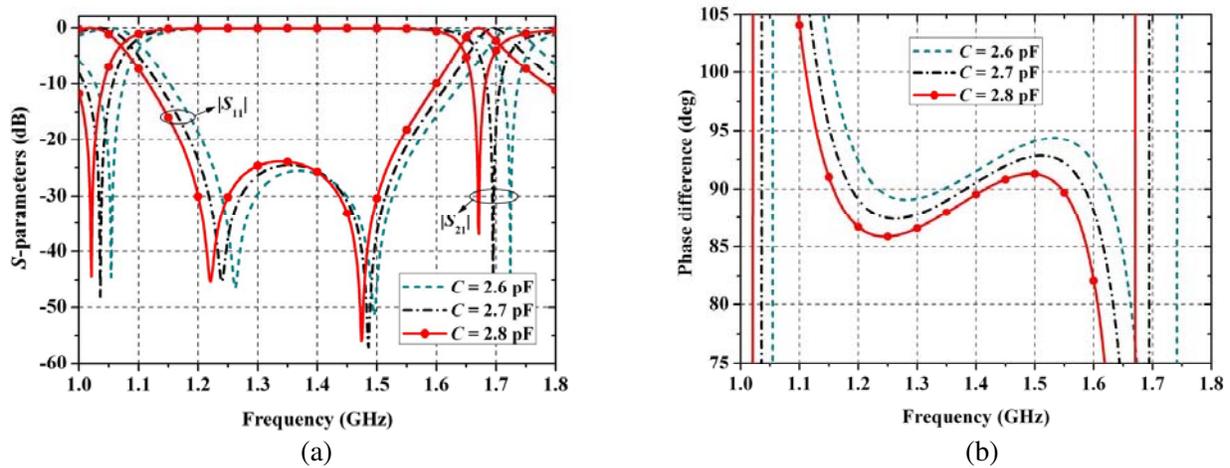
Figure 9. Effect of loaded capacitor on the S-parameters of the proposed $90°$ phase shifter. (a) Amplitude responses. (b) Phase responses.

capacitors with nominal deviation of ± 0.25 pF and the relative dielectric constant ε_r of the substrate with nominal deviation of ± 0.1 in the fabricated prototype, by means of the parametric analysis with HFSS simulation in Figures 9 and 10. Based on the shift of S_{11} (reflection zeros) and S_{21} (transmission zeros) towards lower frequencies in Figures 8(a) and 9(a), the actual value of capacitors used in the fabricated prototype is more than the required value of 2.7 pf. Then, by comparing the phase responses in Figures 9(b) and 10(b) to Figure 8(b), the actual relative dielectric constant of the substrate used in fabricated prototype also is more than the required value of 2.65.

Based on foregoing analysis studies, the following procedures are suggested to design the proposed $90°$ phase shifter.

1) Determine the center frequency, return loss, and impedance bandwidth according to the design requirements. Obtain the values of dielectric constant and thickness of the substrate material.

2) Select proper coupling factor k of the TRD couple line based on the design requirements of return loss at the center frequency and impedance bandwidth referring to Figures 3 and 5.

3) Calculate the impedance Z_{0e1}, Z_{0o1}, and loaded capacitor C of the TRD couple line using Equations (2)–(7).
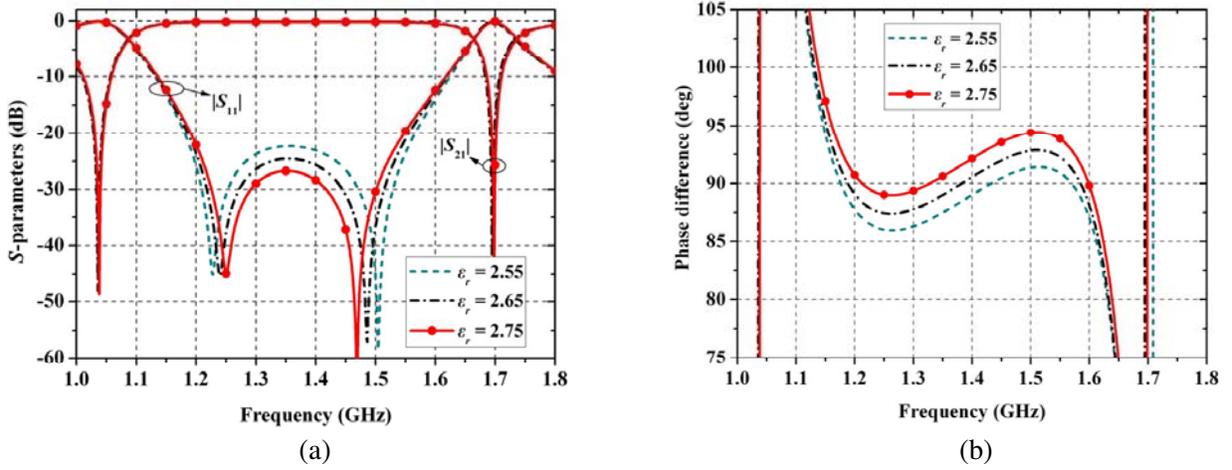
Figure 10. Effect of relative dielectric constant of the substrate on the S-parameters of the proposed 90° phase shifter. (a) Amplitude responses. (b) Phase responses.

4) Choose the even- and odd-mode impedance ratio g of the main coupled line to obtain appropriate phase ripple. Then calculate the impedance Z_{0e2}, Z_{0o2} using the Equations (8) and (12).

5) Convert all the electrical parameters to the physical dimensions.

6) Tune the physical dimensions to obtain the correct phase difference and the available bandwidth using a full-wave electromagnetic simulator. If the proper physical dimensions with the required performance cannot be realized, the design should be restarted from Step 2) with other potential values.

5. CONCLUSIONS

A modified Schiffman phase shifter with an open-circuited $\lambda/4$ TRD coupled line is presented. Compared to the existing 90° Schiffman phase shifter [4–8, 13–19], the reference line of the proposed phase shifter is reduced by two thirds in length, an additional optimization variable added, and two transmission zeros near the operational frequency band achieved with the cost of the maximum realizable bandwidth of about 42%. The parametric analysis and detailed design procedure of the phase shifter are given. The proposed method has been validated with the simulated and measured results. In addition, the proposed phase shifter is suitable for implementation by PCB technology.

ACKNOWLEDGMENT

REFERENCES

1. Liu, Q., Y. Liu, Y. Wu, M. Su, and J. Shen, "Compact wideband circularly polarized patch antenna for CNSS applications," *IEEE Antennas Wirel. Propag. Lett.*, Vol. 12, 1280–1283, 2013.

2. Sun, L., B.-H. Sun, H. Wu, J. Yuan, and W. Tang, "Broadband, wide beam circularly polarized antenna with a novel matching structure for satellite communications," *Progress In Electromagnetics Research C*, Vol. 59, 159–166, 2015.

3. Han, R. C., S. S. Zhong, and J. Liu, "Broadband circularly polarised dielectric resonator antenna fed by wideband switched line coupler," *Electron. Lett.*, Vol. 50, No. 10, 725–726, 2014.

4. Schiffman, B. M., "A new class of broad-band microwave 90-degree phase shifters," *IRE Trans. Microwave Theory Tech.*, Vol. 6, No. 2, 232–237, 1958.

5. Lee, C. H. and Y. H. Chang, "An alternative implementation for fabricating a Schiffman phase shifter," *Microwave Opt. Technol. Lett.*, Vol. 55, No. 1, 9–12, 2013.

6. Guo, Y. X., Z. Y. Zhang, and L. C. Ong, "Improved wide-band Schiffman phase shifter," *IEEE Trans. Microwave Theory Tech.*, Vol. 54, No. 3, 1196–1200, 2006.

7. Rhee, S., "Broadband Schiffman phase shifter using coupled suspended lines with tuning septums," *Microwave Opt. Technol. Lett.*, Vol. 55, No. 5, 1036–1038, 2013.

8. Zhang, Z., Y.-C. Jiao, S.-F. Cao, X.-M. Wang, and F.-S. Zhang, "Modified broadband Schiffman phase shifter using dentate microstrip and patterned ground plane," *Progress In Electromagnetics Research Letters*, Vol. 24, 9–16, 2011.

9. Donelli, M., M. Rukanuzzaman, and C. E. Saavedra, "A methodology for the design of microwave systems and circuits using an evolutionary algorithm," *Progress In Electromagnetics Research M*, Vol. 31, 129–141, 2013.

10. Donelli, M., C. Saavedra, and M. D. Rukanuzzaman, "Design and optimization of a broadband X-band bidirectional amplifier," *Microwave Opt. Technol. Lett.*, Vol. 55, No. 8, 1730–1735, 2013.

11. Azaro, R., G. Boato, M. Donelli, A. Massa, and E. Zeni, "Design of a prefractal monopolar antenna for 3.4–3.6 GHz Wi-Max band portable devices," *IEEE Antennas Wirel. Propag. Lett.*, Vol. 5, 116–119, 2006.

12. Donelli, M. and P. Febvre, "An inexpensive reconfigurable planar array for Wi-Fi applications," *Progress In Electromagnetics Research C*, Vol. 28, 71–81, 2012.

13. Liu, Q., Y. Liu, J. Shen, S. Li, C. Yu, and Y. Lu, "Wideband single-layer $90°$ phase shifter using stepped impedance open stub and coupled-line with weak coupling," *IEEE Microwave Wireless Compon. Lett.*, Vol. 24, No. 3, 176–178, 2014.

14. Liu, Q., H. Liu, and Y. Liu, "Compact ultra-wideband $90°$ phase shifter using short-circuited stub and weak coupled line," *Electron. Lett.*, Vol. 50, No. 20, 1454–1456, 2014.

15. Sorn, M., R. Lech, and J. Mazur, "Simulation and experiment of a compact wideband $90°$ differential phase shifter," *IEEE Trans. Microwave Theory Tech.*, Vol. 60, No. 3, 494–501, 2012.

16. Wang, Y., M. E. Bialkowski, and A. M. Abbosh, "Double microstrip-slot transitions for broadband $±90°$ microstrip phase shifters," *IEEE Microwave Wireless Compon. Lett.*, Vol. 22, No. 2, 58–60, 2012.

17. Eom, S. Y. and H. K. Park, "New switched-network phase shifter with broadband characteristics," *Microwave Opt. Technol. Lett.*, Vol. 38, No. 4, 255–257, 2003.

18. Zheng, S. Y., W. S. Chan, and K. F. Man, "Broadband phase shifter using loaded transmission line," *IEEE Microwave Wireless Compon. Lett.*, Vol. 20, No. 9, 498–500, 2010.

19. Yeung, S. H., Q. Xue, and K. F. Man, "Broadband $90°$ differential phase shifter constructed using a pair of multisection radial line stubs," *IEEE Trans. Microwave Theory Tech.*, Vol. 60, No. 9, 2760–2767, 2012.

20. Zhang, W., Y. Liu, Y. Wu, W. Wang, M. Su, and J. Gao, "A modified coupled-line Schiffman phase shifter with short reference line," *Progress In Electromagnetics Research C*, Vol. 54, 17–27, 2014.

21. Shie, C. I., J. C. Cheng, S. C. Chou, and Y. C. Chiang, "Transdirectional coupled-line couplers implemented by periodical shunt capacitors," *IEEE Trans. Microwave Theory Tech.*, Vol. 57, No. 12, 2981–2988, 2009.

22. Pozar, D. M., *Microwave Engineering*, 4th edition, John Wiley & Sons, New York, 2012.